Silencing of circular RNA-ZYG11B exerts a neuroprotective effect against retinal neurodegeneration

CONG MA[1,2], MU-DI YAO[3,4], XIAO-YAN HAN[3], ZE-HUI SHI[3], BIAO YAN[3] and JIAN-LING DU[1]

Departments of [1]Endocrinology and [2]Ophthalmology, First Affiliated Hospital of Dalian Medical University, Dalian, Liaoning 116011; [3]Eye Institute, Eye & ENT Hospital, Shanghai Medical College, Fudan University, Shanghai 200030; [4]The Fourth School of Clinical Medicine, Nanjing Medical University, Nanjing, Jiangsu 210029, P.R. China

Abstract. Ischemic retinal diseases are the major cause of vision impairment worldwide. Currently, there are no available treatments for ischemia-induced retinal neurodegeneration. Circular RNAs (circRNAs) have emerged as important regulators of several biological processes and human diseases. The present study investigated the role of circRNA-ZYG11B (circ-ZYG11B; hsa_circ_0003739) in retinal neurodegeneration. Reverse transcription quantitative polymerase chain reaction (RT-qPCR) demonstrated that circZYG11B expression was markedly increased during retinal neurodegeneration *in vivo* and *in vitro*. Cell Counting Kit-8, TUNEL and caspase-3 activity assays revealed that silencing of circZYG11B was able to protect against oxidative stress- or hypoxic stress-induced retinal ganglion cell (RGC) injury. Furthermore, immunofluorescence staining and hematoxylin and eosin staining revealed that silencing of circZYG11B alleviated ischemia/reperfusion-induced retinal neurodegeneration, as indicated by reduced RGC injury and decreased retinal reactive gliosis. In addition, luciferase reporter, biotin-coupled miRNA capture and RNA immunoprecipitation assays revealed that circZYG11B could regulate RGC function through circZYG11B/microRNA-620/PTEN signaling. Clinically, RT-qPCR assays demonstrated that circZYG11B expression was markedly increased in the aqueous humor of patients with glaucoma. In conclusion, circZYG11B may be considered a promising target for the diagnosis and treatment of retinal ischemic diseases.

Correspondence to: Professor Biao Yan, Eye Institute, Eye & ENT Hospital, Shanghai Medical College, Fudan University, 83 Fen Yang Road, Shanghai 200030, P.R. China
E-mail: biao.yan@fdeent.org

Dr Jian-Ling Du, Department of Endocrinology, First Affiliated Hospital of Dalian Medical University, 193 Lianhe Road, Dalian, Liaoning 116011, P.R. China
E-mail: dujianlingcn@163.com

Introduction

Retinal ischemia is a major cause of vision loss, which has been implicated in the pathogenesis of several ocular diseases, such as acute angle-closure glaucoma, retinal vascular occlusion and diabetic retinopathy (1,2). Ischemia-induced retinal neurodegeneration is characterized by neural apoptosis, glial activation, abnormal electroretinograms and decreased retinal layer thickness (3,4). Previous studies have revealed that oxidative stress, abnormal neurotrophic factor release, inflammation, metabolic changes and genetic/epigenetic changes are tightly associated with the pathogenesis of retinal neurodegeneration (5,6). Currently, intraocular pressure (IOP)-lowering treatment remains the primary focus of glaucoma management, and anti-angiogenic treatment is the main therapeutic method for diabetic retinopathy management. The established treatment for retinal neurodegeneration is adjunctive neuroprotective therapy for the management of glaucoma or diabetic retinopathy; however, these neuroprotective treatments are only partially or transiently effective as they neither repair the degenerated retinal neurons nor arrest retinal neurodegeneration (7,8) Therefore, further studies are required to identify the mechanism underlying retinal neurodegeneration.

Retinal neurodegeneration is a complicated pathological process, which encompasses a complex interplay of various molecular regulators. Non-coding RNAs account for a large part of the transcriptome and have no protein-coding potential; however, they do generate non-coding transcripts that are involved in numerous biological processes and human diseases (9,10). Circular RNAs (circRNAs) are a group of endogenous RNAs in eukaryotes that are characterized by covalently closed loops with tissue-specific and cell-specific expression patterns (11). Previous studies have shown that circRNAs are involved in the pathogenesis of several neurodegenerative diseases, such as Alzheimer's disease, traumatic brain injury and stroke (12,13). The retina and optic nerve are known as the direct extension of the diencephalon during embryonic development. The brain and the eye have several common characteristics, including a similar vasculature and underlying gene regulatory network (14,15). The present study hypothesized that circRNAs may serve an important role in the pathogenesis of retinal neurodegeneration.

An important facet of retinal ischemic injury is ischemia/reperfusion (I/R) injury. The present study investigated the role of a circRNA in I/R-induced retinal neurodegeneration. circRNA-ZYG11B (circZYG11B; hsa_circ_0003739) is a circRNA located at chr1:53236691-53245665, which has a conserved homologous gene in the mouse genome (mmu_circ_0011029). Moreover, circZYG11B has been reported to be dysregulated in I/R-injured retinas (16). The present study aimed to investigate the effects of circZYG11B silencing on retinal ganglion cell (RGC) injury and I/R-induced retinal neurodegeneration. In addition, it aimed to unveil the molecular mechanisms of circZYG11B-mediated RGC injury and retinal neurodegeneration.

Materials and methods

Primary mouse RGC isolation and culture. A total of 32 C57BL/6J pregnant mice (age, 14 weeks, weight 32-36 g) were purchased from Shanghai SLAC Laboratory Animal Co., Ltd. and maintained in our laboratory at a controlled temperature of $23\pm2°C$ and a relative humidity of $50\pm10\%$ under a 12-h light/dark cycle with free access to food and water. For RGC isolation, approximately eight postnatal day 5 mice were used. Mice were anesthetized with a mixture of ketamine (80 mg/kg) and xylazine (4 mg/kg), and then euthanized in a chamber via 100% CO_2 exposure at a displacement rate of 50% volume/min for 50 min (17). After euthanasia, the eyes were immediately enucleated in cold dissection buffer containing HBSS (cat. no. 14025134; Gibco; Thermo Fisher Scientific, Inc.) and 2 mM HEPES (cat. no. H3784; MilliporeSigma). Subsequently, the retinas were separated from the sclera and pigment epithelium under a binocular dissecting microscope (MZ7.5; Leica Microsystems GmbH). The retinas were placed in dissection buffer and digested with 5 mg/ml papain for 0.5 h at 37°C. The suspensions of retinal cells were incubated with anti-macrophage antiserum (1:100; cat. no. AIA31240; Accurate Chemical & Scientific Corporation) for 1 h at 37°C to eliminate macrophages and microglial cells. The non-adherent cells were transferred to 100-mm petri dishes pre-conjugated with anti-Thy1.2 antibody (pre-conjugation for 3 h at room temperature; 1:20 dilution; cat. no. MCA02R; Bio-Rad Laboratories, Inc) to purify RGCs for 1 h at 37°C. The dishes were then rinsed with PBS to remove the non-adherent cells. The adherent cells were released using trypsin (cat. no. T4799; MilliporeSigma) and triturated with a pipette. RGCs were cultured in DMEM (cat. no. 21013024; Gibco; Thermo Fisher Scientific, Inc.) supplemented with insulin (2.0 mM; cat. no. I6634; MilliporeSigma), progesterone (40 nM; cat. no. P0130; MilliporeSigma), selenite (60 nM; cat. no. S5261; MilliporeSigma), transferrin (100 nM; cat. no. T8158; MilliporeSigma), CNTF (40 ng/ml; cat. no. 450-13; PeproTech, Inc.) and forskolin (6 μM; cat. no. F6886; MilliporeSigma) at 37°C and in an atmosphere containing 5% CO_2. For hypoxic induction, RGCs were cultured in a NAPCO 7001 incubator (The Precision Scientific Company) containing 1% O_2, 5% CO_2 and 94% N_2 at 37°C for 24 h. For oxidative stress induction, RGCs were exposed to H_2O_2 (50 μM) to mimic oxidative stress at 37°C for 24 h. The group without hypoxic induction or oxidative stress induction was taken as the control group.

Cell Counting Kit (CCK)-8 assay. The viability of RGCs was determined by CCK-8 assays (cat. no. CK04; Dojindo Laboratories, Inc.) according to the manufacturer's protocol. Briefly, 5x10^3 RGCs/well were seeded into a 96-well plate. After transfection and exposure to hypoxic stress or oxidative stress, RGCs were incubated with 20 μl CCK-8 solution in each well for 3 h at 37°C. The absorbance was then detected at a wavelength of 450 nm using a microplate reader (Molecular Devices, LLC).

Caspase-3 activity assay. Caspase-3 activity was determined using the caspase-3 assay kit (cat. no. C1168S; Beyotime Institute of Biotechnology) according to the manufacturer's protocol. Briefly, RGCs were cultured at a density of 5x10^3 cells/well in a 96-well plate. After the required treatment, cells were incubated with 100 μl caspase-3 substrate/well for 1 h at 37°C. Caspase-3 activity was determined under 490 nm excitation wavelength and 525 nm emission wavelength. Values were obtained from the blank group (caspase 3 substrate and cell culture medium, without RGCs) and subtracted from the experimental group values. The change in caspase-3 activity was calculated relative to the value obtained from the untreated cell group. Each sample was measured in duplicate.

Retinal I/R injury model. A total of 35 male C57BL/6 mice (age, 8 weeks; weight, 25-30 g) were used for detecting circZYG11B expression change during retinal neurodegeneration and investigating the role of circZYG11B in retinal neurodegeneration. The mice were purchased from Shanghai SLAC Laboratory Animal Co., Ltd. The mice were housed in a pathogen-free environment (temperature, $23\pm2°C$; humidity, $50\pm5\%$) under a 12-h light/dark cycle with free access to food and water. All operations were conducted under anesthesia via an intraperitoneal injection of ketamine (80 mg/kg) and xylazine (4 mg/kg) (18,19). During I/R injury, the body temperature was maintained at 37°C using a temperature-controlled heating pad. The pupils were dilated using 0.5% phenylephrine and 0.5% tropicamide (Santen). Oxybuprocaine hydrochloride (Santen) was then applied to the corneas, followed by injection with a 30-gauge needle connected to a sterile bag containing 0.9% sodium chloride. To detect circZYG11B expression changes during I/R-induced retinal neurodegeneration, the anterior chamber of one eye was cannulated with a 30-gauge needle connected to the saline bag, which was located 120 cm above the eye, leading to a high IOP of ~90 mmHg. After removing the needle from the anterior chamber for 1 h, the IOP returned to normal. The contralateral eye was connected to the saline bag, which was not raised above the eye, thus a normal IOP was maintained as the control. The needle was withdrawn from the eye after 1 h. The retinas were collected at 0, 3 and 7 days after I/R injury (n=5 mice/time point).

To investigate whether silencing of circZYG11B affected retinal neurodegeneration, the mice were randomly separated into the following four groups: i) Control group: One eye was injected with the needle without elevating IOP and the other eye was left untreated (n=5 mice); ii) I/R group: One eye underwent I/R injury and the other eye was left untreated (n=5 mice); iii) I/R + control shRNA group: One eye was injected with scrambled (Scr) short hairpin (sh)RNA and underwent I/R injury and the other eye was left untreated (n=5 mice);

and iv) I/R + circZYG11B shRNA: One eye was injected with circZYG11B shRNA and underwent I/R injury and the other eye was left untreated (n=5 mice). A total of 7 days after I/R injury, the mice were euthanized in a chamber via 100% CO_2 exposure at a displacement rate of 50% volume/min. The mice received an intravitreous injection of 1.0 μl (7.5x10^{-5} μg/ml) circZYG11B shRNA or equal amounts of Scr shRNA 14 days before I/R injury. The mice were injected once and sacrificed 21 days after injection. The sequence for circZYG11B shRNA was 5'-GGACACTTGAAGGAGGAAGCCTTCAAGAGA GGCTTCCTCCTTCAAGTGTCCTTTTTG-3'; the sequence for negative control shRNA was 5'-TCCTAAGGTTAAGTC GCCCTCGCTCGAGCGAGGGCGACTTAACCTTAGGTT TTTG-3'. The shRNAs (OBio Technology) were inserted into an AAV-2 vector (Stratagene; Agilent Technologies, Inc.) under the control of RNA polymerase III promoter U6, and then packaged with pHelper and pAAV-RC to produce recombinant AAV2-circZYG11B shRNA or AAV2-Scr shRNA. The target site for circZYG11B shRNA was located at the junctional site of circZYG11B spanning 9 nt sequence on one side and 12 nt on the other side.

Cell transfection. RGCs were cultured onto 6-well plates at 37˚C overnight at a density of 1x10^5 cells/well. When cell confluence had reached 80%, RGCs were transfected with circZYG11B small interfering (si)RNA, negative control siRNA, Scr mimic, miR-620 mimic, pcDNA 3.1 (Vector) or PTEN-pcDNA 3.1 (all purchased from Sangon Biotech Co., Ltd.) using Lipo6000™ transfection reagent (cat. no. C0526; Beyotime Institute of Biotechnology) according to the manufacturer's protocol. circZYG11B siRNA, negative control siRNA, Scr mimic, miR-620 mimic, pcDNA 3.1 and PTEN-pcDNA 3.1 were diluted in Opti-MEM (Gibco; Thermo Fisher Scientific, Inc.), added to a culture plate and mixed gently 3-5 times. Lipo6000™ transfection reagent was also diluted in Opti-MEM and incubated for 5 min at room temperature. Subsequently, the diluted siRNA, mimics or plasmids, and transfection reagent were combined and incubated at room temperature for 20 min. The mixture was then added to each well for transfection. After 12 h at 37˚C, the medium was replaced and cells were cultured at 37˚C for an additional 12 h for the subsequent experiments. The sequences were as follows: circZYG11B siRNA, sense 5'-GGACACUUGAAG GAGGAAGCCTdTd-3', anti-sense 5'-GGCUUCCUCCUUCA AGUGUCCUdTdTd-3'; Scr siRNA, sense 5'-UUCUCCGAA CGUGUCACGUTdTd-3', anti-sense 5'-ACGUGACACGUU CGGAGAATdTdT-3'; miR-620 mimic, 5'-AUGGAGAUA GAUAUAGAAAUU-3'; negative control miRNA mimic, 5'-UCGCUUGGUGCAGGUCGGG-3'. During transfection, the concentration of miRNA mimics and siRNAs was 50 nM, and the concentration of plasmids was 4.0 μg.

Hematoxylin and eosin (H&E) staining. Eyes obtained from the four groups of mice were enucleated and fixed in 4% paraformaldehyde at 4˚C overnight. The eyes were then dehydrated in graded concentrations of ethanol and embedded in paraffin. Sections (5 μm) were cut vertically through the optic nerve head. Subsequently, the paraffin-embedded tissue sections were dewaxed with xylene and rehydrated in graded concentrations of ethanol. After washing with ddH$_2$O, the sections were stained with hematoxylin for 5 min at room temperature, stained with eosin for 45 sec at room temperature, and mounted with neutral resin at room temperature for long-term storage (cat. no. C0105S; Beyotime Institute of Biotechnology). The images were captured using an Olympus IX-73 bright-field microscope (Olympus Corporation).

Immunofluorescence staining. The retinas were dissected in PBS and fixed in 4% paraformaldehyde for 12 h at room temperature. Subsequently, they were immersed in 30% sucrose solution for another 12 h and embedded in optimum cutting temperature compound mounting media. Sections (10 μm) were cut and placed on gelatin-coated slides. After rehydration with PBS, retinal sections were blocked with 5% bovine serum albumin (cat. no. ST025; Beyotime Institute of Biotechnology) for 30 min at 37˚C to minimize nonspecific labeling. Retinal sections were incubated with primary antibodies against GFAP (1:200; cat. no. ab7260; Abcam), NeuN (1:300; cat. no. ab128886; Abcam) or anti-tubulin β3 (TUJ1; 1:300; cat. no. 801213; Biolegend, Inc.) overnight at 4˚C. The slides were then washed with PBS containing 0.1% Tween 20 and incubated with Alexa Fluor 594 8 secondary antibodies (1:500; cat. nos. ab150080 and ab150116; Abcam) overnight at 4˚C. After washing with PBS, the nuclei were labeled with DAPI (cat. no. D9542; MilliporeSigma) for 15 min at room temperature. The staining signaling was observed in six selected visual fields using an Olympus IX-73 fluorescence microscope (Olympus Corporation). Adobe Photoshop CS2 (Adobe Systems, Inc.) software was used for the preprocessing the fluorescent images.

TUNEL staining assay. The apoptosis of RGCs was determined using the TUNEL Apoptosis Detection kit (cat. no. C11026; Guangzhou RiboBio Co., Ltd.) according to the manufacturer's protocol. RGCs were fixed with 4% paraformaldehyde at 4˚C for 30 min and were blocked with the blocking buffer (3% H_2O_2 in CH_3OH) at room temperature for 15 min. Subsequently, RGCs were permeabilized with 0.1% Triton X-100 for 10 min on ice, incubated with the TUNEL reaction mixture for 1 h at 37˚C and stained with DAPI for 5 min at room temperature to label cell nuclei. The staining signaling was observed in six selected visual fields using an Olympus IX-73 fluorescence microscope (Olympus Corporation).

Luciferase reporter assay. circZYG11B sequence was inserted into the *Kpn*I and *Hind*III sites of pGL3 vector (Promega Corporation) to generate the Luc-circZYG11B vector. circZYG11B-interacting miRNAs were predicted using the circular RNA Interactome database (https://circinteractome. nia.nih.gov/) (20). RGCs were seeded in 96-well plates at a density of 5x10^3 cells/well. After 24 h culture, RGCs were transfected with different miRNA mimics (final concentration: 50 nM) using Lipo6000™ transfection reagent according to the manufacturer's protocol. After 12 h, the medium was replaced and RGCs were cultured at 37˚C for additional 12 h for luciferase activity assay. All miRNA mimics were synthesized by Sangon Biotech Co., Ltd. The mRNA mimics used were as follows: miR-149 mimic, 5'-UCUGGCUCCGUG UCUUCACUCCCUU-3'; miR-186 mimic, 5'-CAAAGAAUU CUCCUUUUGGGCUUU-3'; miR-543 mimic, 5'-AAACAU UCGCGGUGCACUUCUUUU-3'; miR-545 mimic, 5'-UCA

GCAAACAUUUAUUGUGUGCUU-3'; miR-568 mimic, 5'-AUGUAUAAAUGUAUACACACUU-3'; miR-607 mimic, 5'-GUUCAAAUCCAGAUCUAUAACUU-3'; miR-616 mimic, 5'-AGUCAUUGGAGGGUUUGAGCAGUU-3'; miR-587 mimic, 5'-UUUCCAUAGGUGAUGAGUCAC UU-3'; miR-620 mimic, 5'-AUGGAGAUAGAUAUAGAA AUUU-3'; miR-624 mimic, 5'-CACAAGGUAUUGGUAUUA CCUUU-3'; miR-634 mimic, 5'-AACCAGCACCCCAAC UUUGGACUU-3'; miR-654 mimic, 5'-UGGUGGGCCGCA GAACAUGUGCUU-3'; miR-936 mimic, 5'-ACAGUAGAG GGAGGAAUCGCAGUU-3'; miR-95 mimic, 5'-UCAAUA AAUGUCUGUUGAAUUUU-3'; The luciferase activity was detected using a Dual-Luciferase Reporter Assay kit (Promega Corporation). The vector pRL-TK expressing *Renilla* luciferase was used as the internal control for transfection. The empty vector pGL3-basic was used as the negative control. For comparisons, the luciferase activity of the pGL3 vector was normalized with *Renilla* luciferase activity.

Biotin-coupled miRNA capture. RGCs (~1x10^6) were transfected with biotinylated miR-620 mimics (5'-AUGGAGAUA GAUAUAGAAAUUU-3') or control mimics (miR-95 mimic: 5'-UCAAUAAAUGUCUGUUGAAUUUU-3'), which were synthesized by Sangon Biotech Co., Ltd., using Lipo6000™ transfection reagent according to the manufacturer's protocol. The final concentration of miRNA mimics was 50 nM. After transfection for 24 h, the cells were lysed in 500 μl lysis buffer (50 mM Tris-HCl, pH 7.5; 150 mM NaCl; 1% Triton X-100; 1% sodium deoxycholate; 0.1% SDS). Subsequently, 50 μl washed streptavidin magnetic beads (Thermo Fisher Scientific, Inc.) were blocked in 1% bovine serum albumin (cat. no. ST025; Beyotime Institute of Biotechnology) for 2 h (21). These beads were then added to the reaction tubes and incubated with 300 μl lysates for 3 h at 4°C to pull down the biotin-coupled RNA complex. After washing the beads with ice-cold lysis buffer, RNA was isolated with TRIzol® reagent (cat. no. 15596018; Invitrogen; Thermo Fisher Scientific, Inc.) and the expression levels of circZYG11B and circZNF236 (negative control) were detected by reverse transcription-quantitative PCR (RT-qPCR).

RNA immunoprecipitation (RIP) assay. RIP assays were conducted using the EZ-Magna RIP kit (MilliporeSigma) according to the manufacturer's protocol. Briefly, RGCs were lysed in the RIP lysis buffer and the cell lysate was incubated with magnetic beads conjugated with anti-Ago2 or anti-IgG antibody for 8 h at 4°C. The beads were then incubated with proteinase K (Invitrogen; Thermo Fisher Scientific, Inc.) for 30 min at 58°C to remove proteins. Finally, the immunoprecipitated RNAs were extracted using TRIzol reagent according to the manufacturer's instructions and subjected for RT-qPCR to determine the expression levels of circZYG11B.

Target gene prediction. The target gene information of miR-620 was predicted using TargetScan software (http://www.targetscan.org/) (22).

RT-qPCR. Total RNAs were extracted from retinal tissues or RGCs using TRIzol reagent according to the manufacturer's instructions. For mRNA expression detection, total RNAs were reverse transcribed using the SuperScript III first-strand

Table I. List of quantitative PCR primers.

Gene	Sequences (5'-3')
Mouse circZYG11B	F: CTTGCCCAATCTTGTGTCCC
	R: CAGGGTTCCATCTTGGCGT
Mouse ZYG11B	F: AACTTTCTCCCGCCTTTCCA
	R: TGTGTCCTAAAGAGGCACCC
Human circZYG11B	F: GGGCATTCTTTGTTCGGGAA
	R: CACCTGTGGCATCAAGTTCC
Human ZYG11B	F: CCCACTGTCAAATTCTCACTGAC
	R: GCCATAGTGAGAACAGTGCCT
Mouse PTEN	F: AGGATACGCGCTTGGGC
	R: ACAGCGGCTCAACTCTCAAA
Human GAPDH	F: AAGACGGGCGGAGAGAAACC
	R: CGTTGACTCCGACCTTCACC
Mouse GAPDH	F: AGGTCGGTGTGAACGGATTTG
	R: TGTAGACCATGTAGTTGAGGTCA
miR-620	F: GCCGAGATGGAGATAGATAT
	R: CTCAACTGG TGTCGTGGA
U6	F: CTCGCTTCGGCAGCACATATACT
	R: ACGCTTCACGAATTTGCGTGTC

circZYG11B, circular RNA ZYG11B; miR, microRNA.

synthesis kit (Invitrogen; Thermo Fisher Scientific, Inc.) according to the manufacturer's protocol. The temperature protocols for RT were as follows: 37°C for 60 min, 95°C for 5 min and maintenance at 4°C. Subsequently, qPCR assays were conducted using the PowerUp™ SYBR™ Green Master Mix (cat. no. A25742; Applied Biosystems; Thermo Fisher Scientific, Inc.) in a PikoReal 96 cycler (Thermo Fisher Scientific, Inc.) using gene-specific primers (Table I) according to the manufacturer's protocol. The thermocycling protocols were as follows: Initial denaturation at 95°C for 3 min, followed by 42 cycles at 95°C for 10 sec, 56°C for 30 sec and 72°C for 30 sec, followed by final extension at 72°C for 60 sec. GAPDH was used as a housekeeping gene.

For miR-620 detection, RT was conducted using the miScript Reverse Transcription kit (Qiagen GmbH) according to the manufacturer's protocol in a final volume of 20 μl containing 5 μl total RNA, 5 μl 5X miScript RT buffer and 1 μl miScript Reverse Transcriptase Mix. The temperature protocols for RT were as follows: 37°C for 60 min, at 95°C for 5 min and maintenance at 4°C. qPCR was conducted using the miScript SYBR-Green PCR kit (Qiagen GmbH) in a PikoReal 96 cycler (Thermo Fisher Scientific, Inc.) using gene-specific primers (Table I) according to the manufacturer's protocol. The thermocycling protocols were as follows: Initial denaturation at 95°C for 3 min, followed by 42 cycles at 95°C for 10 sec, 56°C for 30 sec and 72°C for 30 sec, followed by final extension at 72°C for 60 sec. Small nuclear RNA U6 was used as a housekeeping gene. Relative mRNA or miR-620 expression was calculated using the 2$^{-\Delta\Delta Cq}$ method (23).

Clinical sample collection. Aqueous humor (AH) samples were obtained from Eye & ENT Hospital (Shanghai, China)
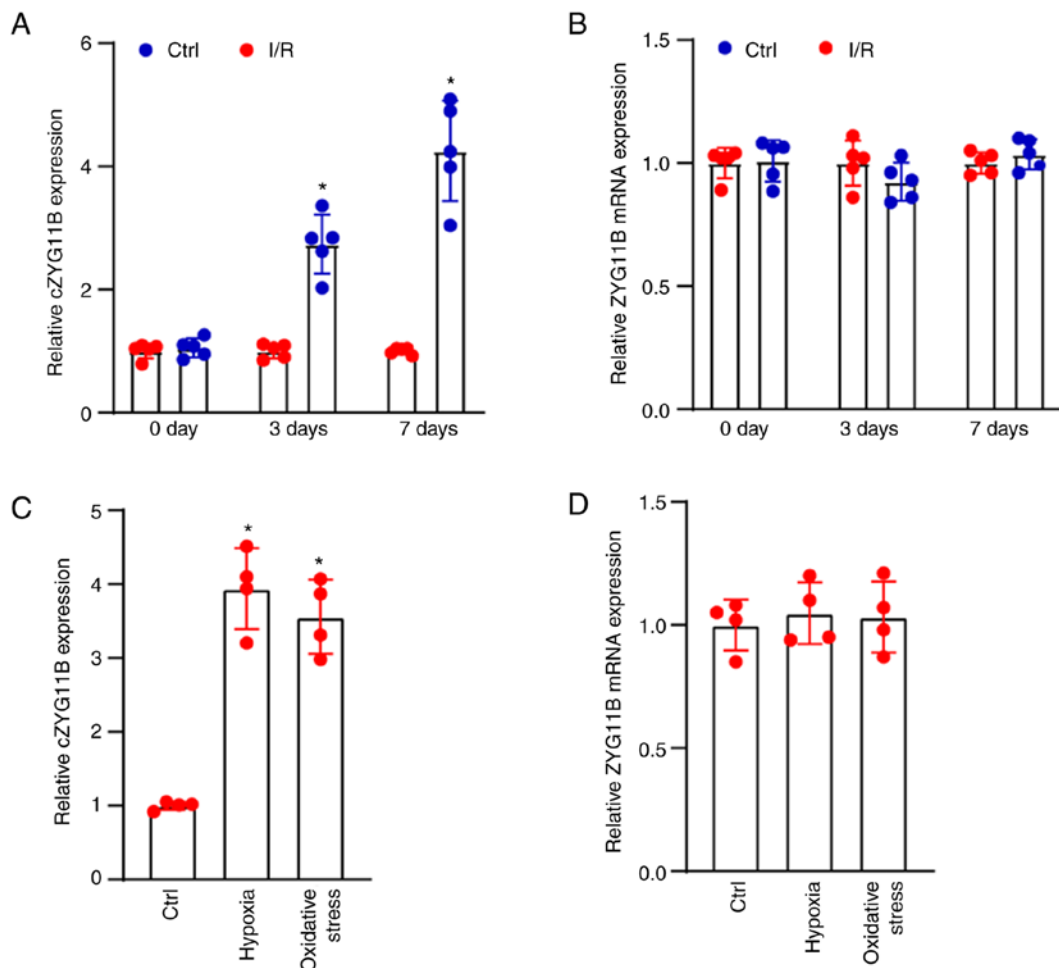
Figure 1. cZYG11B expression is increased during I/R-induced retinal neurodegeneration *in vivo* and *in vitro*. RT-qPCR was conducted to detect the expression levels of (A) cZYG11B and (B) ZYG11B mRNA in the normal (Ctrl) and I/R retinas at day 0, 3 or 7 after I/R injury. n=5. *P<0.05 vs. Ctrl group, paired Student's t-test. Isolated retinal ganglion cells were untreated (Ctrl), or were exposed to H_2O_2 (50 μmol/l) or 1% O_2 to mimic oxidative stress or hypoxic stress, respectively. RT-qPCR was conducted to detect the expression levels of (C) cZYG11B and (D) ZYG11B mRNA 24 h after injury. *P<0.05 vs. Ctrl group, one-way ANOVA followed by Bonferroni post hoc test. n=4. Ctrl, control; cZYG11B, circZYG11B; RT-qPCR, reverse transcription-quantitative PCR.

between November 2018 and March 2019. Written informed consent was obtained from the patients involved. Glaucoma AH samples were obtained from patients diagnosed with acute angle-closure glaucoma (12 male and eight female patients; age range, 53-66 years). Control AH samples were obtained from patients diagnosed with cataracts without acute angle-closure glaucoma (11 male and nine female patients; age range, 50-63 years). The patients were diagnosed at the hospital through ocular examination, including anterior segment photography, Goldmann applanation tonometry, fundus examination, visual field, optic disc photography and ultrasound biomicroscopy examination. The patients with glaucoma were diagnosed as having acute angle-closure glaucoma without cataracts and required filtration surgery. Patients were excluded if they had other ophthalmic or systemic diseases, had accepted systemic and local steroids therapy for glaucoma treatment, or had accepted ophthalmic surgery or intravitreous injections of anti-VEGF drugs.

ELISA. The levels of PTEN in AH samples were determined using a human PTEN ELISA Kit (cat. no. ab206979; Abcam) according to the manufacturer's protocol. Briefly, the standard samples and AH samples were added to the pre-coated

96-well plates and incubated for 1 h at room temperature, followed by the addition of the antibody cocktail to each well. Subsequently, the plates were sealed and incubated for 1 h at room temperature. After washing the plates three times, the TMB Development Solution was added to each well and incubated for 10 min in the dark on a plate shaker set to 400 rpm. Finally, the Stop Solution was added to each well to terminate the enzyme-substrate reaction. After the reaction was terminated for 3 min, the absorbance value of each well was measured at a wavelength of 450 nm. A standard curve was plotted for determining the concentration of PTEN in each sample. All measurements were performed in duplicate.

Statistical analysis. All data were analyzed using GraphPad Prism 5 (GraphPad Software, Inc.). The experiments were independently repeated three times and the data are presented as the mean ± standard deviation. Comparisons between two independent samples were analyzed using the paired Student's t-test (Comparison of circZYG11B expression between I/R retinas and normal retinas) or unpaired Student's t-test (comparison of circZYG11B, miR-620 and PTEN levels in AH samples between patients with glaucoma and patients with cataracts), and multiple comparisons were made using
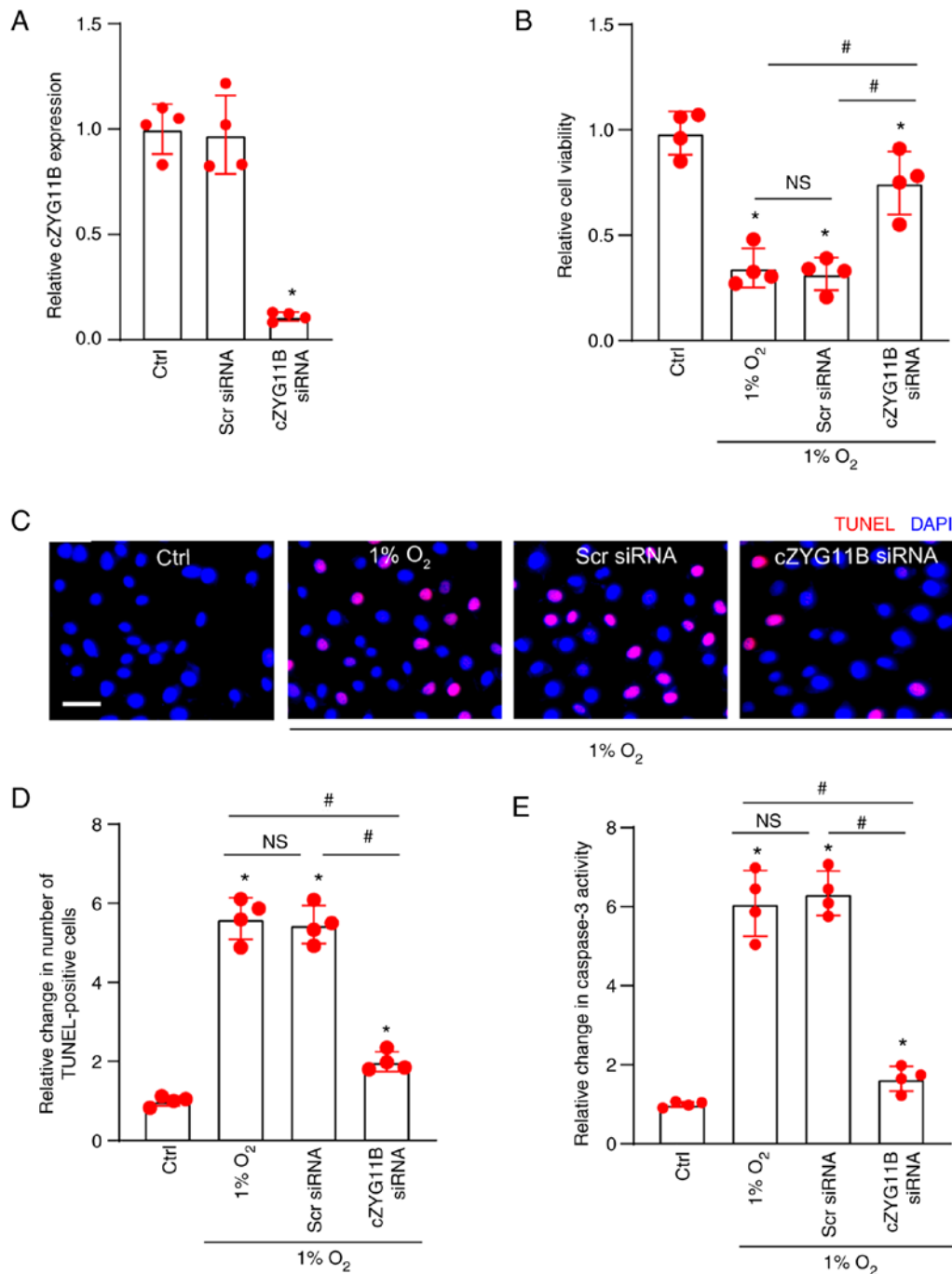
Figure 2. Silencing of cZYG11B alleviates hypoxic stress-induced RGC injury. (A) RGCs were transfected with Scr siRNA or cZYG11B siRNA for 12 h. The medium was replaced and cultured for an additional 12 h at 37°C. The untransfected group was used as a Ctrl. Reverse transcription-quantitative PCR was conducted to detect the expression levels of cZYG11B. (B-E) RGCs were transfected and then exposed to 1% O_2 to mimic hypoxic stress for 24 h at 37°C. The Ctrl group was not transfected nor exposed to 1% O_2 exposure. (B) Cell Counting Kit-8 assays were conducted to detect the viability of RGCs. (C and D) TUNEL staining assays and quantification analysis was performed to detect the apoptosis of RGCs upon hypoxic stress (scale bar, 50 μm). (E) Caspase-3 activity was detected to evaluate the degree of RGC apoptosis upon hypoxic stress. *P<0.05 vs. Ctrl group; #P<0.05 as indicated; NS, no significant difference; one-way ANOVA followed by the Bonferroni post hoc test. n=4. Ctrl, control; cZYG11B, circZYG11B; RGC, retinal ganglion cell; Scr, scrambled; siRNA, small interfering RNA.

one-way ANOVA followed by Bonferroni's test. P<0.05 was considered to indicate a statistically significant difference.

Results

circZYG11B expression is increased during I/R-induced retinal neurodegeneration in vivo and in vitro. Models of retinal I/R injury are important for studying retinal

neurodegeneration (16). Retinal I/R injury was induced by an acute increase in IOP. The present study used a mouse model of retinal I/R injury and detected the expression levels of circ-ZYG11B between I/R retinas and control retinas. IOP in one eye was raised to ~90 mm Hg for 1 h, and the contralateral eye was cannulated and maintained at normal IOP as the control. The needle was withdrawn from the eye after 1 h. The mice were sacrificed at 0, 3 and 7 days after I/R injury. The results
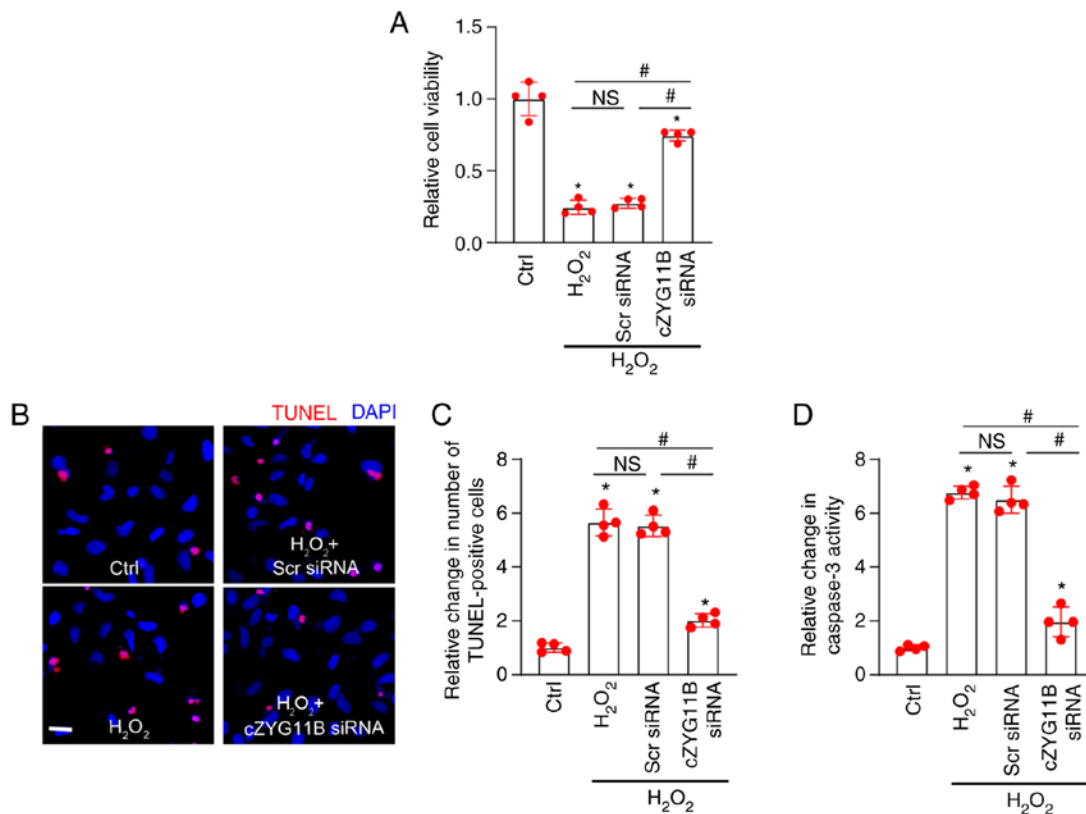
Figure 3. Silencing cZYG11B alleviates oxidative stress-induced RGC injury. RGCs were transfected with Scr siRNA, cZYG11B siRNA or left untreated for 12 h. The medium was replaced and cultured for an additional 12 h at 37°C. They were then exposed to H_2O_2 (50 μmol/l) to mimic oxidative stress for 24 h at 37°C. The Ctrl group was nt transfected nor exposed to H_2O_2. (A) Cell Counting Kit-8 assays were conducted to detect the viability of RGCs. (B and C) TUNEL staining assays and quantification analysis was performed to detect the apoptosis of RGCs upon oxidative stress (scale bar, 50 μm). (D) Caspase 3 activity was detected to evaluate the degree of RGC apoptosis upon oxidative stress. $^*P<0.05$ vs. Ctrl group; $^\#P<0.05$ as indicated; NS, no significant difference; one-way ANOVA followed by the Bonferroni post hoc test. n=4. Ctrl, control; cZYG11B, circZYG11B; RGC, retinal ganglion cell; Scr, scrambled; siRNA, small interfering RNA.

demonstrated that circZYG11B was significantly increased in the retinas at day 3 or day 7 after I/R injury (Fig. 1A). By contrast, the mRNA expression levels of ZYG11B were not altered in the retinas after I/R injury (Fig. 1B). Retinal neurons, particularly RGCs, have been shown to be highly sensitive to I/R injury (3). In the present study, the isolated RGCs were exposed to H_2O_2 (50 μM) or 1% O_2 at 37°C for 24 h to mimic oxidative stress or hypoxic stress. The group without exposure to H_2O_2 or 1% O_2 was taken as the control group. The results revealed that compared with in the control group, exposure to H_2O_2 or 1% O_2 increased the expression levels of circZYG11B. By contrast, exposure to H_2O_2 or 1% O_2 did not alter the mRNA expression levels of ZYG11B (Fig. 1C and D).

Silencing of circZYG11B alleviates hypoxic stress-induced RGC injury. The present study then investigated the role of circZYG11B in RGCs *in vitro*. RT-qPCR confirmed that transfection with circZYG11B siRNA decreased the expression levels of circZYG11B compared with in the control group (Fig. 2A). Hypoxic stress is an important pathological factor in retinal I/R injury (24). The non-transfected RGCs, or RGCs transfected with circZYG11B siRNA or Scr siRNA were exposed to 1% O_2 to mimic hypoxic stress *in vitro*. The non-transfected RGCs without 1% O_2 treatment was taken as the control group. CCK-8 assays revealed that compared with in the control group without 1% O_2 exposure, hypoxic stress induced by 1% O_2 led to decreased RGC viability. Compared

with the 1% O_2 group, transfection of circZYG11B siRNA, but not Scr siRNA, significantly alleviated hypoxic stress-induced reduction of RGC viability (Fig. 2B). TUNEL assays revealed that compared with the control group without 1% O_2 exposure, 1% O_2 treatment led to an increased number of apoptotic RGCs. The number of apoptotic RGCs in the circZYG11B group was lower than that in the 1% O_2 group or in the 1% O_2 + Scr siRNA group (Fig. 2C and D). Caspase-3 activity assays revealed that hypoxic stress enhanced the activity of caspase-3. Compared with in the 1% O_2 group, transfection with circZYG11B siRNA, but not Scr siRNA, reduced the activity of caspase-3 induced by hypoxic stress (Fig. 2E). Collectively, silencing of circZYG11B may have a protective role in RGCs against hypoxic stress.

Silencing of circZYG11B alleviates oxidative stress-induced RGC injury. Oxidative stress is another pathological factor in retinal I/R injury (24). The non-transfected RGCs or RGCs transfected with circZYG11B siRNA or Scr siRNA were exposed to H_2O_2 (50 μmol/l) to mimic oxidative stress *in vitro*. CCK-8 assays revealed that compared with in the control group without H_2O_2 exposure, H_2O_2 treatment-mediated oxidative stress led to reduced viability of RGCs. Compared with in the H_2O_2 group, transfection with circZYG11B siRNA, but not Scr siRNA, alleviated the oxidative stress-induced reduction of RGC viability (Fig. 3A). TUNEL assays revealed that compared with in the control group without H_2O_2 exposure,
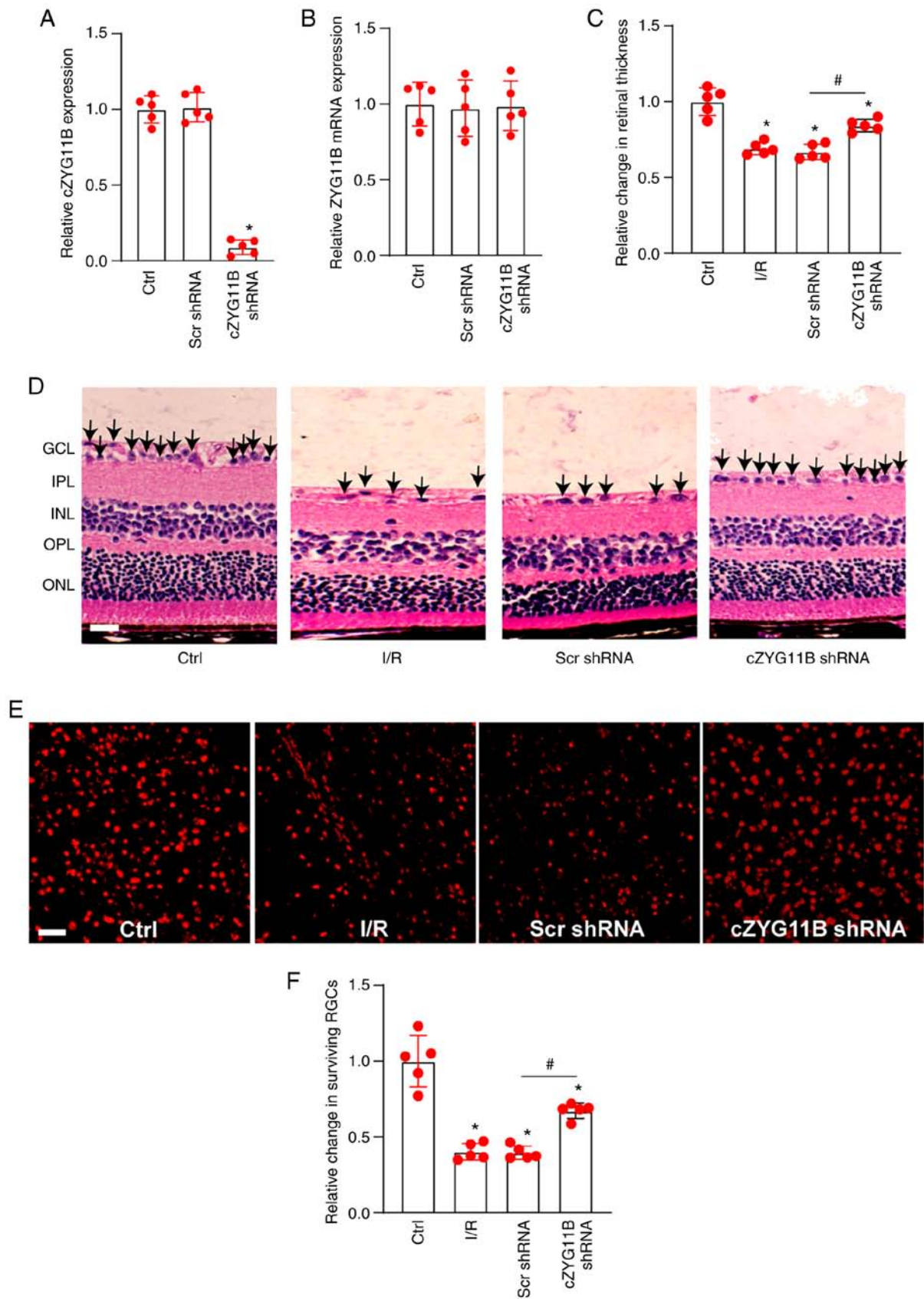
Figure 4. Silencing of cZYG11B alleviates I/R-induced retinal injury *in vivo*. (A and B) C57BL/6 mice received an intravitreous injection of cZYG11B shRNA, Scr shRNA or were untreated for 7 days. Reverse transcription-quantitative PCR was conducted to detect the expression levels of (A) cZYG11B and (B) ZYG11B mRNA. (C and D) Hematoxylin and eosin staining of retinal sections and semi-quantification analysis was conducted to detect changes in retinal thickness in normal retinas (Ctrl), I/R retinas, I/R retinas injected with Scr shRNA or I/R retinas injected with cZYG11B shRNA. Scale bar, 50 μm. Arrows indicate the nuclei of RGCs. (E and F) Normal retinas (Ctrl), I/R retinas, I/R retinas injected with Scr shRNA or I/R retinas injected with cZYG11B shRNA were stained with TUJ1 to label the surviving RGCs at day 7 after I/R injury. Scale bar, 20 μm. *P<0.05 vs. Ctrl group; $^\#$P<0.05 as indicated; Kruskal-Wallis test followed by the post hoc Bonferroni test. n=5. Ctrl, control; cZYG11B, circZYG11B; I/R, ischemia/reperfusion; RGC, retinal ganglion cell; Scr, scrambled; shRNA, short hairpin RNA; GCL, ganglion cell layer; IPL, inner plexiform layer; INL, inner nuclear layer; OPL, outer plexiform layer; ONL, outer nuclear layer.
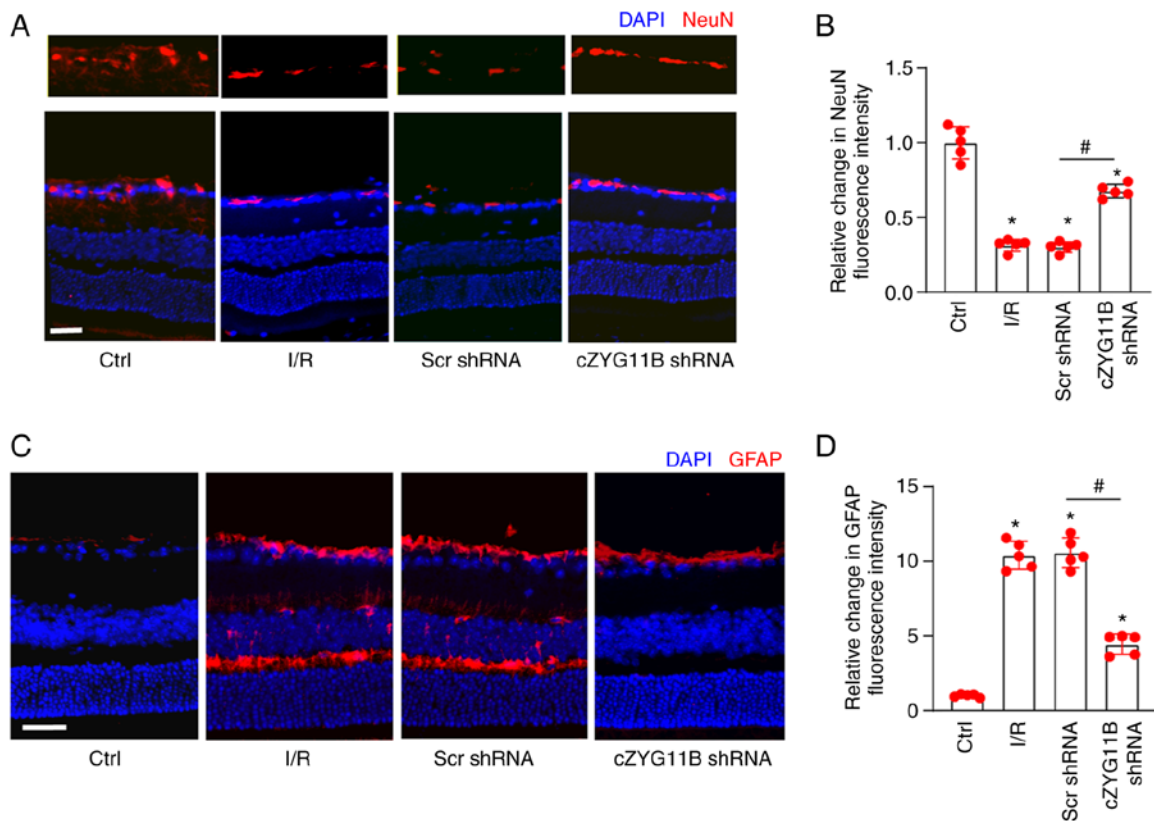
Figure 5. Silencing of cZYG11B suppresses I/R-induced RGC injury and retinal reactive gliosis *in vivo*. (A-D) Mice received an intravitreal injection of cZYG11B shRNA or Scr shRNA. A total of 3 weeks after intravitreal injection, I/R model was constructed to study retinal neurodegeneration. Immunofluorescence staining with (A and B) NeuN or (C and D) GFAP was conducted to detect retinal neurodegeneration at day 7 after I/R injury. The representative images and semi-quantitative results were shown. Nuclei, blue; NeuN-positive cells, red; GFAP-positive cells, red. Scale bar, 50 μm. *P<0.05 vs. Ctrl group; #P<0.05 as indicated; Kruskal-Wallis test followed by the post hoc Bonferroni test. n=5. Ctrl, control; cZYG11B, circZYG11B; I/R, ischemia/reperfusion; RGC, retinal ganglion cell; Scr, scrambled; shRNA, short hairpin RNA.

treatment with H_2O_2 (50 μmol/l) led to an increased number of apoptotic RGCs. However, the number of apoptotic RGCs was significantly decreased post-transfection with circZYG11B siRNA, but not Scr siRNA (Fig. 3B). Oxidative stress led to enhanced caspase-3 activity in RGCs. Compared with in the H_2O_2 group, transfection with circZYG11B siRNA, but not Scr siRNA, significantly decreased the activity of caspase-3 induced by H_2O_2 (Fig. 3C). These findings suggested that silencing of circZYG11B could exert protective effects on RGCs against oxidative stress.

Silencing of circZYG11B alleviates I/R-induced retinal injury in vivo. The present study next determined the role of circ-ZYG11B in I/R-induced retinal injury *in vivo*. C57BL/6 mice received an intravitreous injection of circZYG11B shRNA to knockdown the expression of circZYG11B. Injection with circZYG11B shRNA significantly reduced the expression levels of circZYG11B compared with in the control group, but did not alter the mRNA expression levels of ZYG11B in the retinas (Fig. 4A and B). H&E staining revealed that silencing of circZYG11B could partially reverse the reduction in I/R injury-induced retinal thickness and reduce I/R-induced neurodegeneration in the ganglion cell layer (GCL) (Fig. 4C and 4D). Retinas were also extracted and the surviving RGCs were quantified at day 7 after I/R injury. The density of surviving RGCs in the I/R group was decreased by ~40%

compared with in the control group. Silencing of circZYG11B exerted protective effects on RGC survival and protected against I/R-induced RGC injury (Fig. 4E and F).

Silencing of circZYG11B suppresses I/R-induced RGC injury and retinal reactive gliosis. The present study further determined the role of circZYG11B in I/R-induced retinal degeneration *in vivo*. Immunofluorescence staining with NeuN was conducted to identify RGCs in the GCL. Compared with in the control retinas, I/R injury led to reduced expression of NeuN. Compared with in the Scr shRNA-injected retinas, injection of circZYG11B shRNA alleviated I/R-induced RGC injury as shown by increased NeuN staining (Fig. 5A and B). The retinas were then stained with GFAP to detect retinal reactive gliosis. Compared with in the control retinas, I/R injury led to activation of retinal reactive gliosis. Silencing of circZYG11B could alleviate I/R-induced retinal reactive gliosis as shown by decreased GFAP staining (Fig. 5C and D). These findings indicated that circZYG11B silencing could alleviate I/R-induced retinal neurodegeneration.

circZYG11B regulates RGC function by acting as a miR-620 sponge. The present study next investigated the underlying mechanism of circZYG11B in retinal neurodegeneration. The Ago2 protein is a core component of the RNA-induced silencing complex that binds miRNA complexes to target genes.
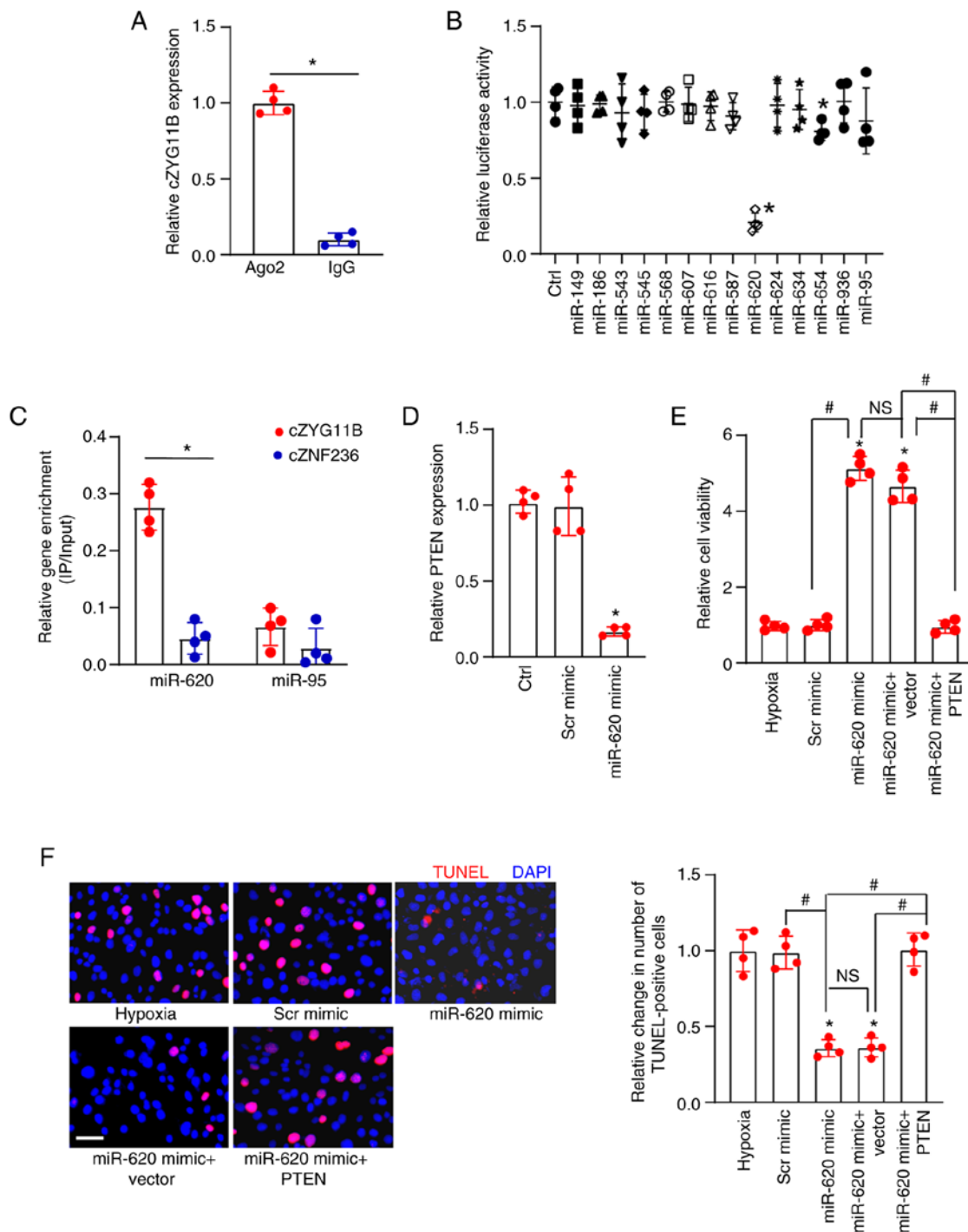
Figure 6. cZYG11B regulates RGC function by acting as a miR-620 sponge. (A) Total cellular fractions were isolated from RGCs and immunoprecipitated using Ago2 or IgG antibody. The amount of cZYG11B in the IP was determined by RT-qPCR. *P<0.05 as indicated. (B) RGCs were transfected with pGL3-Basic (Ctrl) or Luc-cZYG11B with various miRNA mimics and pRL-TK vector (internal transfection control). Luciferase activity was detected at 24 h post-transfection using the Dual-Luciferase Reporter Assay kit. *P<0.05 vs. Ctrl. (C) Biotinylated miR-620 or miR-95 were transfected into RGCs. After streptavidin capture, the amount of cZYG11B and cZNF236 (negative control) in the input and bound fractions were detected by RT-qPCR. The relative IP/input ratios were plotted. *P<0.05 as indicated. (D) RGCs were transfected with Scr mimic, miR-620 mimic or were untreated. RT-qPCR was conducted to detect PTEN expression. *P<0.05 vs. Ctrl. (E and F) RGCs were left untreated or transfected with Scr mimic, miR-620 mimic, miR-620 mimic + pcDNA 3.1 (Vector) or PTEN-pcDNA 3.1 (PTEN) for 12 h. The medium was replaced and cells were cultured for an additional 12 h at 37˚C. These groups were then exposed to 1% O$_2$ to mimic hypoxic stress for 24 h at 37˚C. (E) CCK-8 assays were conducted to detect the viability of RGCs. (F) TUNEL staining assays and semi-quantification analysis were conducted to detect the apoptosis of RGCs. Scale bar, 50 µm. *P<0.05 vs. hypoxia group; #P<0.05 as indicated; NS, no significant difference. All significant differences were evaluated by (A and C) Student's t-test or (B, D-F) one-way ANOVA followed by the post hoc Bonferroni test. n=4. Ctrl, control; cZYG11B, circZYG11B; IP, immunoprecipitated; miR, microRNA; RGC, retinal ganglion cell; RT-qPCR, reverse transcription-quantitative PCR; Scr, scrambled.

miRNAs associate with the Ago2 protein to post-transcriptionally suppress target gene expression (20). The RIP assays indicated that circZYG11B could be pulled down by Ago2 antibody but not IgG, suggesting that circZYG11B may serve a role by acting as a miRNA sponge (Fig. 6A). Luciferase activity assay demonstrated that transfection with miR-620 mimics or
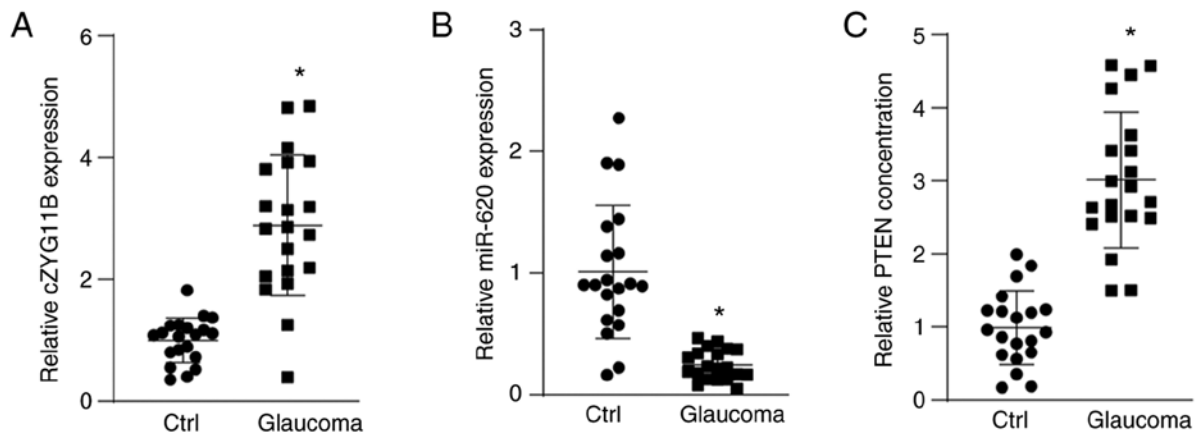
Figure 7. Clinical relevance of cZYG11B-mediated signaling in I/R-related ocular disease. Aqueous humor samples were collected from patients with glaucoma (n=20) and patients with cataracts (Ctrl; n=20). Reverse transcription-quantitative PCR was conducted to detect the expression levels of (A) cZYG11B and (B) miR-620. (C) ELISA was conducted to detect the concentration of PTEN. The significant differences were determined by unpaired Student's t-test. *P<0.05 vs. Ctrl group. Ctrl, control; cZYG11B, circZYG11B; miR, microRNA.

miR-654 mimics, but not the other miRNA mimics, reduced the activity of Luc-circZYG11B (Fig. 6B). Due to the greater silencing efficiency of miR-620 compared with miR-654 on the activity of Luc-circZYG11B, the present study focused on the role of miR-620 in RGCs. Because miR-95 mimics did not reduce the luciferase activity of Luc-circZYG11B, it was suggested that miR-95 could not directly bind to circZYG11B; therefore, miR-95 was selected as the negative control for RNA pull-down assays. RNA pull-down assays revealed that circZYG11B but not circZNF236 was greatly enriched in the miR-620-captured fraction. By contrast, there was no difference between the amount of circZYG11B and circZNF236 in the miR-95-captured fraction (negative control) (Fig. 6C). Subsequently, the potential target genes of miR-620 were predicted using TargetScan software (http://www.targetscan.org/) (22). The candidate gene, PTEN, was assessed further due to its role in cell apoptosis.

RT-qPCR revealed that transfection with a miR-620 mimic led to increased expression of miR-620 but decreased expression of PTEN (Figs. S1 and 6D). The present study then investigated the role of miR-620 in RGC biology *in vitro*. All experimental groups were exposed to 1% O$_2$ to mimic hypoxic stress. The non-transfected group was taken as the control group (hypoxia group). CCK-8 and TUNEL assays demonstrated that compared with in the control group, transfection with the miR-620 mimic, but not Scr mimic, led to increased cell viability and reduced number of TUNEL-positive cells, thus suggesting that the miR-620 mimic exerted protective effects on RGC function (Fig. 6E and F). Western blotting demonstrated that transfection with pcDNA3.1-PTEN increased the protein expression levels of PTEN in RGCs (Fig. S2). Notably, overexpression of PTEN could interrupt the protective effects of miR-620 on RGC function (Fig. 6E and F). Collectively, these results suggested that circZYG11B may regulate RGC function via the circZYG11B/miR-620/PTEN signaling axis.

Clinical relevance of circZYG11B-mediated signaling in I/R-related ocular disease. The present study also investigated the clinical significance of circZYG11B-mediated signaling. Acute angle-closure glaucoma is an I/R-related ocular disease (23). AH samples were collected from patients with glaucoma (n=20) and patients with cataracts (control; n=20). circZYG11B expression was significantly higher in the AH samples from patients with glaucoma compared with that in control patients (Fig. 7A). By contrast, miR-620 expression was significantly downregulated in the AH samples from patients with glaucoma compared with control patients (Fig. 7B). The concentrations of PTEN in AH samples were determined using ELISA. The results revealed that PTEN concentration was markedly increased in the AH samples of patients with glaucoma compared with the control patients, showing a similar pattern as circZYG11B (Fig. 7C). Collectively, these results suggested that circZYG11B-mediated signaling is potentially involved in I/R-related ocular disease.

Discussion

Retinal ischemia is a major cause of vision impairment and a common pathological basis of several ocular diseases, including glaucoma, diabetic retinopathy and central retinal artery occlusion (25). Prevention of I/R injury could slow the development of retinal neurodegeneration (26). The present study demonstrated that silencing of circZYG11B could reduce retinal reactive gliosis and decrease RGC injury *in vivo*. Knockdown of circZYG11B could also alleviate hypoxic stress- and oxidative stress-induced RGC injury. The present study provides a novel circRNA-mediated mechanism underlying retinal ischemic diseases.

Retinal I/R injury is involved in a wide spectrum of pathological conditions, such as retinal neurodegeneration and retinal vascular dysfunction (25). Previous studies have shown that this process is regulated by a complex regulatory network, including coding RNAs and non-coding RNAs (27-29). circRNAs are a novel class of endogenous non-coding RNA generated by back-splicing, which have emerged as novel regulators of gene expression and are known to be involved in the pathogenesis of diabetic retinopathy, glaucoma and central retinal artery occlusion (30-33). Therefore, circRNAs have been highlighted as promising biomarkers for the diagnosis and assessment of disease progression and prognosis. The

present study demonstrated that circZYG11B was significantly upregulated during retinal neurodegeneration *in vivo* and *in vitro*. Acute angle-closure glaucoma is an I/R-related ocular disease, and in the present study, circZYG11B expression levels were significantly upregulated in the AH samples of patients with glaucoma compared with those in the control patients with cataracts. circZYG11B-mediated signaling was also dysregulated in I/R-related ocular disease. Thus, circZYG11B may be considered a promising biomarker for the diagnosis and prognosis of retinal I/R-related diseases.

I/R-related retinal diseases are major causes of vision impairment worldwide and there are currently no available treatments (34). Oxidative stress and hypoxic stress are the key drivers of disease progression and RGC injury during retinal I/R (35). I/R injury can lead to the production of reactive oxygen species, inflammation and retinal injury, including vascular injury and neurodegeneration. Retinal neurons, particularly RGCs, are highly sensitive to retinal ischemia (25,36). In response to hypoxic or oxidative stress, silencing of circ-ZYG11B could protect RGCs against the relevant injuries *in vitro*. Moreover, knockdown of circZYG11B could alleviate I/R injury-induced retinal neurodegeneration *in vivo*. Thus, circZYG11B silencing may be a promising neuroprotective strategy for the treatment of I/R-related ocular diseases.

Previous studies have shown that circRNAs generated from exons often reside in the cytoplasm and may act as miRNA sponges (37,38). The present study demonstrated that circ-ZYG11B could bind to miR-620 and regulate RGC function by acting as a miRNA sponge. circZYG11B acted as a binding platform for Ago2 and miR-620. Notably, PTEN was veri-fied as a target gene of miR-620; PTEN has been reported to act as a mediator of apoptosis and to have an important role in neurons (39,40). In hippocampal cells, knockdown of PTEN has been shown to significantly protect against staurosporine-induced apoptosis as shown, by decreased reactive oxygen species production, reduced release of cytochrome *c* and decreased activation of caspase 9 (39). PTEN is normally localized in the cytosol, and can be recruited to specific microdomains of the plasma membrane and contribute to the development of lactacystin-induced neuronal apoptosis (40). In prostate cancer cells, PTEN was able to suppress constitutive Akt activation and enhance cell apoptosis. PTEN could also sensitize cells to death receptor-mediated apoptosis and non-receptor mediated apoptosis (41). Overexpression of PTEN could also sensitize prostate cells to cell death induced by staurosporine, doxorubicin and vincristine. By contrast, loss of PTEN could enhance the mRNA and protein expression levels of Bcl-2, an anti-apoptotic protein, leading to decreased death in prostate cancer cells (42). Therefore, circZYG11B could act as a sponge for miR-620, thus releasing the suppressive effect of miR-620 on PTEN. This regulatory mechanism could provide a novel insight into RGC injury and I/R-induced retinal neurodegeneration.

In conclusion, the present study investigated the expression pattern of circZYG11B and the relevant mechanism in I/R-induced retinal neurodegeneration. The results revealed that circZYG11B was increased in retinal neurodegeneration *in vivo* and *in vitro*. By contrast, silencing of circZYG11B could protect against I/R-induced RGC injury and alleviate I/R-induced retinal neurodegeneration. The present study provides a novel perspective on the mechanism of retinal I/R injury and a potential target for treating I/R-related ocular diseases.

Availability of data and materials

The datasets used and/or analyzed during the current study are available from the corresponding author on reasonable request.

Authors' contributions

BY and JLD designed the study. CM, MDY, ZHS and XYH conducted the experiments, and participated in the design, statistics, drafting and revising of the manuscript. CM, MDY and ZHS analyzed the data. All authors read and approved the final manuscript. BY and JLD confirm the authenticity of all the raw data.

Ethics approval and consent to participate

The animals were maintained according to the guidelines of the Care and Use of Laboratory Animals (published by the National Institutes of Health) (43) and handled according to the ARVO Statement for the Use of Animals in Ophthalmic and Vision Research (44). Animal experiments were approved by the Animal Care and Use Committee of Eye & ENT Hospital. Clinical experiments were approved by the Ethics Committee of Eye & ENT hospital. Written informed consent was received from the patients involved.

Patient consent for publication

Not applicable.

Competing interests

The authors declare that they have no competing interests.

References

1. Piano I, Di Paolo M, Corsi F, Piragine E, Bisti S, Gargini C and Di Marco S: Retinal neurodegeneration: Correlation between nutraceutical treatment and animal model. Nutrients 13: 770, 2021.
2. Usategui-Martin R and Fernandez-Bueno I: Neuroprotective therapy for retinal neurodegenerative diseases by stem cell secretome. Neural Regen Res 16: 117-118, 2021.
3. Carrasco E, Hernández C, Miralles A, Huguet P, Farrés J and Simó R: Lower somatostatin expression is an early event in diabetic retinopathy and is associated with retinal neurodegeneration. Diabetes Care 30: 2902-2908, 2007.
4. Carrasco E, Hernández C, de Torres I, Farrés J and Simó R: Lowered cortistatin expression is an early event in the human diabetic retina and is associated with apoptosis and glial activation. Mol Vis 14: 1496-1502, 2008.

5. Fukumoto M, Nakaizumi A, Zhang T, Lentz SI, Shibata M and Puro DG: Vulnerability of the retinal microvasculature to oxidative stress: Ion channel-dependent mechanisms. Am J Physiol Cell Physiol 302: C1413-C1420, 2012.

6. Kowluru RA, Engerman RL, Case GL and Kern TS: Retinal glutamate in diabetes and effect of antioxidants. Neurochem Int 38: 385-390, 2001.

7. Baltmr A, Duggan J, Nizari S, Salt TE and Cordeiro MF: Neuroprotection in glaucoma-Is there a future role? Exp Eye Res 91: 554-566, 2010.

8. Simó R, Stitt AW and Gardner TW: Neurodegeneration in diabetic retinopathy: Does it really matter? Diabetologia 61: 1902-1912, 2018.

9. Zelinger L and Swaroop A: RNA biology in retinal development and disease. Trends Genet 34: 341-351, 2018.

10. Song J and Kim YK: Targeting non-coding RNAs for the treatment of retinal diseases. Mol Ther Nucleic Acids 24: 284-293, 2021.

11. Kristensen LS, Andersen MS, Stagsted LV, Ebbesen KK, Hansen TB and Kjems J: The biogenesis, biology and characterization of circular RNAs. Nat Rev Genet 20: 675-691, 2019.

12. Beermann J, Piccoli MT, Viereck J and Thum T: Non-coding RNAs in development and disease: Background, mechanisms, and therapeutic approaches. Physiol Rev 96: 1297-1325, 2016.

13. Esteller M: Non-coding RNAs in human disease. Nat Rev Genet 12: 861-874, 2011.

14. Cheung CY, Ikram MK, Chen C and Wong TY: Imaging retina to study dementia and stroke. Prog Retin Eye Res 57: 89-107, 2017.

15. Jiang Q, Su DY, Wang ZZ, Liu C, Sun YN, Cheng H, Li XM and Yan B: Retina as a window to cerebral dysfunction following studies with circRNA signature during neurodegeneration. Theranostics 11: 1814-1827, 2021.

16. Yao MD, Zhu Y, Zhang QY, Zhang HY, Li XM, Jiang Q and Yan B: CircRNA expression profile and functional analysis in retinal ischemia-reperfusion injury. Genomics 113: 1482-1490, 2021.

17. Pritchett K, Corrow D, Stockwell J and Smith A: Euthanasia of neonatal mice with carbon dioxide. Comp Med 55: 275-281, 2005.

18. Zhang J, Sio SW, Moochhala S and Bhatia M: Role of hydrogen sulfide in severe burn injury-induced inflammation in mice. Mol Med 16: 417-424, 2010.

19. Bae GS, Park KC, Choi SB, Jo IJ, Choi MO, Hong SH, Song K, Song HJ and Park SJ: Protective effects of alpha-pinene in mice with cerulein-induced acute pancreatitis. Life Sci 91: 866-871, 2012.

20. Dudekula DB, Panda AC, Grammatikakis I, De S, Abdelmohsen K and Gorospe M: CircInteractome: A web tool for exploring circular RNAs and their interacting proteins and microRNAs. RNA Biol 13: 34-42, 2016.

21. Jiang L, Luirink J, Kooijmans SA, van Kessel KP, Jong W, van Essen M, Seinen CW, de Maat S, de Jong OG, Gitz-François JF, et al: A post-insertion strategy for surface functionalization of bacterial and mammalian cell-derived extracellular vesicles. Biochim Biophys Acta Gen Subj 1865: 129763, 2021.

22. Witkos TM, Koscianska E and Krzyzosiak WJ: Practical aspects of microRNA target prediction. Curr Mol Med 11: 93-109, 2011.

23. Livak KJ and Schmittgen TD: Analysis of relative gene expression data using real-time quantitative PCR and the 2(-Delta Delta C(T)) method. Methods 25: 402-408, 2001.

24. Li SY, Fu ZJ and Lo AC: Hypoxia-induced oxidative stress in ischemic retinopathy. Oxid Med Cell Longev 2012: 426769, 2012.

25. Osborne NN, Casson RJ, Wood JP, Chidlow G, Graham M and Melena J: Retinal ischemia: Mechanisms of damage and potential therapeutic strategies. Prog Retin Eye Res 23: 91-147, 2004.

26. Tezel G: Oxidative stress in glaucomatous neurodegeneration: Mechanisms and consequences. Prog Retin Eye Res 25: 490-513, 2006.

27. Wan P, Su W, Zhang Y, Li Z, Deng C, Li J, Jiang N, Huang S, Long E and Zhuo Y: LncRNA H19 initiates microglial pyroptosis and neuronal death in retinal ischemia/reperfusion injury. Cell Death Differ 27: 176-191, 2020.

28. Ge Y, Zhang R, Feng Y and Li H: Mbd2 mediates retinal cell apoptosis by targeting the lncRNA Mbd2-AL1/miR-188-3p/Traf3 axis in ischemia/reperfusion injury. Mol Ther Nucleic Acids 19: 1250-1265, 2020.

29. Ghafouri-Fard S, Shoorei H and Taheri M: Non-coding RNAs participate in the ischemia-reperfusion injury. Biomed Pharmacother 129: 110419, 2020.

30. Cui G, Wang L and Huang W: Circular RNA HIPK3 regulates human lens epithelial cell dysfunction by targeting the miR-221-3p/PI3K/AKT pathway in age-related cataract. Exp Eye Res 198: 108128, 2020.

31. Wu PC, Zhang DY, Geng YY, Li R and Zhang YN: Circular RNA-ZNF609 regulates corneal neovascularization by acting as a sponge of miR-184. Exp Eye Res 192: 107937, 2020.

32. Guo N, Liu XF, Pant OP, Zhou DD, Hao JL and Lu CW: Circular RNAs: Novel promising biomarkers in ocular diseases. Int J Med Sci 16: 513-518, 2019.

33. Liu C, Ge HM, Liu BH, Dong R, Shan K, Chen X, Yao MD, Li XM, Yao J, Zhou RM, et al: Targeting pericyte-endothelial cell crosstalk by circular RNA-cPWWP2A inhibition aggravates diabetes-induced microvascular dysfunction. Proc Natl Acad Sci USA 116: 7455-7464, 2019.

34. Biousse V, Nahab F and Newman NJ: Management of acute retinal ischemia: Follow the guidelines! Ophthalmology 125: 1597-1607, 2018.

35. Fortmann SD and Grant MB: Molecular mechanisms of retinal ischemia. Curr Opin Physiol 7: 41-48, 2019.

36. Neufeld AH, Kawai Si, Das S, Vora S, Gachie E, Connor JR and Manning PT: Loss of retinal ganglion cells following retinal ischemia: The role of inducible nitric oxide synthase. Exp Eye Res 75: 521-528, 2002.

37. Kulcheski FR, Christoff AP and Margis R: Circular RNAs are miRNA sponges and can be used as a new class of biomarker. J Biotechnol 238: 42-51, 2016.

38. Lavenniah A, Luu TD, Li YP, Lim TB, Jiang J, Ackers-Johnson M and Foo RS: Engineered circular RNA sponges act as miRNA inhibitors to attenuate pressure overload-induced cardiac hypertrophy. Mol Ther 28: 1506-1517, 2020.

39. Zhu Y, Hoell P, Ahlemeyer B and Krieglstein J: PTEN: A crucial mediator of mitochondria-dependent apoptosis. Apoptosis 11: 197-207, 2006.

40. Choy MS, Bay BH, Cheng HC and Cheung NS: PTEN is recruited to specific microdomains of the plasma membrane during lactacystin-induced neuronal apoptosis. Neurosci Lett 405: 120-125, 2006.

41. Yuan XJ and Whang YE: PTEN sensitizes prostate cancer cells to death receptor-mediated and drug-induced apoptosis through a FADD-dependent pathway. Oncogene 21: 319-327, 2002.

42. Huang H, Cheville JC, Pan Y, Roche PC, Schmidt LJ and Tindall DJ: PTEN induces chemosensitivity in PTEN-mutated prostate cancer cells by suppression of Bcl-2 expression. J Biol Chem 276: 38830-38836, 2001.

43. National Research Council (US): Committee for the update of the guide for the care and use of laboratory animals: Guide for the care and use of laboratory animals. 8th edition. National Academies Press, Washington, DC, 2011.

44. Seitz R, Hackl S, Seibuchner T, Tamm ER and Ohlmann A: Norrin mediates neuroprotective effects on retinal ganglion cells via activation of the Wnt/beta-catenin signaling pathway and the induction of neuroprotective growth factors in Muller cells. J Neurosci 30: 5998-6010, 2010.